



Estimation of Actual Evapotranspiration Using Soil Moisture Balance and Remote Sensing

Dewu Huang¹ · Jianying Wang² · Majid Khayatnezhad³

Received: 9 September 2020 / Accepted: 16 December 2020 / Published online: 10 January 2021
© Shiraz University 2021

Abstract

Determination of actual evapotranspiration is an important step for simulating the crop growth models in agricultural decision-making process. In this study, actual evapotranspiration (ET_a) values for the main crops cultivated in Shahrekord plain, Chaharmahal and Bakhtiari province, Iran, are estimated based on real-time modeling and compared with the results obtained from the remote sensing data. Soil moisture balance was simulated considering the variation rate of crop canopy cover and its effects on evaporation and transpiration parameters. Daily values of ET_a were predicted in a repeatable cycle based on the available soil moisture in root zone. Moreover, remote sensing images were analyzed as a data source to achieve the crop water requirement in critical times. For this objective, surface energy balance algorithm for land (SEBAL) was used to characterize the evapotranspiration and then derived ET_a. Preliminary results obtained by applying satellite information showed a good agreement between the SEBAL estimates of evapotranspiration fluxes and the corresponding values simulated by the soil moisture estimation technique.

Keywords Remote sensing · Soil moisture · SEBAL · Agriculture · Canopy cover

1 Introduction

As the competition for the finite water resources on earth increases due to growth in population and affluence, agriculture is faced with intensifying pressure to improve the efficiency of water used for food production (Hsiao et al. 2007; Yao et al. 2018; Mason 2019). Therefore, in increasing population growth, rapid development in agriculture and growing scarcity of water resources, much of the studies have focused on water tension management (Lalehzari et al. 2020), water delivery scheduling (Omidzade et al. 2020), groundwater level monitoring (Fry et al. 2020), efficient allocation of water resources (Yan et al. 2020), and resolving conflicts between water consumers (Lalehzari and Kerachian 2020; Li and Kinzelbach 2020). Irrigation agriculture

is one of the large consumers of water in arid and semi-arid regions which its allocation affects directly the yield production, food security, and system efficiency (Fallah-Mehdipour et al. 2013; Sun et al. 2017; Li and Kinzelbach 2020). The sustainable management of water resources in agriculture is often accompanied by the development of simulation models based on the crop growth patterns or estimating the irrigation water requirement (Yan et al. 2018; Sang et al. 2019; Varzi et al. 2019).

Evapotranspiration is an important factor in irrigation water planning and crop water tension monitoring (Li and Kinzelbach 2020). However, direct measurement of actual evapotranspiration is difficult and, at best, mostly provides point values (Akbari et al. 2007; Reyes-Acosta and Lubczynski 2011; Balugani et al. 2017). Actual evapotranspiration (ET_a) of plants has been considered as a main factor of decision system in different studies (Parsinejad et al. 2013; Li and Kinzelbach 2020), which is estimated by various procedures such as remote sensing (Mahan et al. 2012; Colak et al. 2015; Veysi et al. 2017), crop water stress index (Lalehzari et al. 2016) and soil moisture balance (Vedula et al. 2005; Balugani et al. 2016; Maroufpoor et al. 2019; Lalehzari and Kerachian 2020).

✉ Jianying Wang
ynwangjianying@163.com

¹ City College, Kunming University of Science and Technology, Kunming 650051, Yunnan, China

² Engineering School, Yunnan University of Business Management, Kunming 650106, Yunnan, China

³ Young Researchers Club, Ardabil Branch, Islamic Azad University, Ardabil, Iran

At present, satellite remote sensing data can be used to estimate actual and potential evapotranspiration in real time at regional scale (Chen et al. 2005; Ines et al. 2006). Moreover, predicting the evapotranspiration based on the satellite images would be helpful to reduce uncertainty in the simulated parameters of the agricultural system and soil water budget (Irmak and Kamble 2009). The main advantages of remote sensing application in agriculture are the high level of covered area and obtainable data without extensive monitoring networks (Chemin et al. 2004; Akbari et al. 2007). Various algorithms have been developed to utilize the satellite observations for quantifying evapotranspiration by different researchers (Allen et al. 2007; Irmak and Kamble 2009; Veysi et al. 2017).

Water shortage in Iran requires the development and evaluation of different decision-making strategies appropriate for irrigation planning to improve production, reduce water consumption and make optimal use of water. Due to the impact of soil water balance on evaporation, transpiration, and water use efficiency, the soil water balance (SWB) was simulated for 13 crops in Shahrekord plain, Iran. Crop growth modeling and soil moisture balance are provided using real-time programming in MATLAB software. Furthermore, SEBAL technique is incorporated as an efficient tool to estimate the actual evapotranspiration in the studied crops for considering the accuracy of predicted results.

2 Materials and Methods

2.1 Soil Water Balance (SWB)

The main structure of the modeling process to estimate the actual evapotranspiration has been summarized in Fig. 1. In the first step, soil water balance (SWB) was formulated in daily time steps by transpiration (Tr), evaporation (E), deep percolation (DP), irrigation (I), and rainfall (R) components, and the water stored in root zone. Therefore, the soil moisture balance in the root zone could be defined as following equation:

$$\Delta S = I + R - E - Tr - DP \quad (1)$$

where ΔS = the change of the moisture storage in the root zone (mm). As shown in Fig. 1, simulating the crop growth was carried out to achieve the daily values of canopy cover and transpiration (Tr).

$$Tr = Kc \times K_{sw} \times K_{cs} \times ET_o \quad (2)$$

where Kc = the crop transpiration coefficient that is addressed as a proportional ratio to the fraction of the soil surface covered by canopy cover, K_{sw} = the soil water stress coefficient which is smaller than 1, K_{cs} = the cold stress

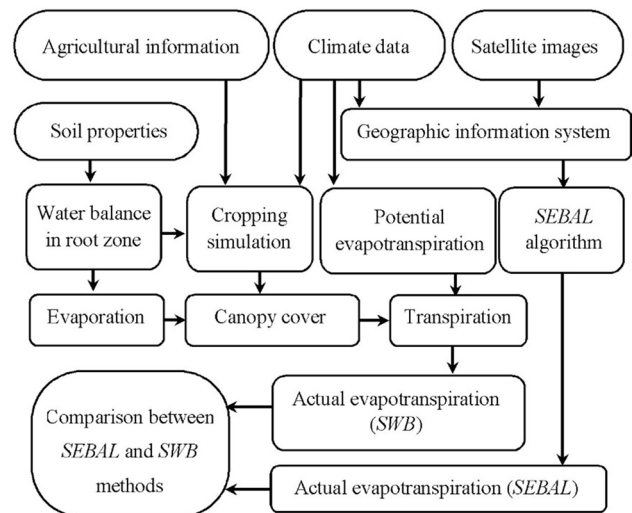


Fig. 1 Schematic of simulation–optimization model

coefficient which becomes smaller than 1 when there are not enough growing degrees in the day.

The evaporation (E) in Eq. (1) was estimated by multiplying the daily potential evapotranspiration with three reduction factors (Raes et al. 2017).

$$E = Kr \times \left(\sqrt[4]{\frac{RAW_E + 1}{20}} \right) \times (1 - Kc) \times ET_o \quad (3)$$

where Kr = the evaporation reduction coefficient which becomes $0 \leq Kr \leq 1$; REW = readily allowable water for evaporation (mm) and $(1 - Kc)$ could be defined as soil evaporation coefficient. In Eq. (3), Kr reduces soil evaporation rate when insufficient moisture is available in the root zone to the evaporative demand.

To determine the calibrated values of effective rainfall, a daily soil water balance incorporating crop transpiration, evaporation, irrigation, rainfall, and the storage capacity of the root zone was used. Hence, by considering the daily potential evapotranspiration and rainfall, the daily effective rainfall (R_E) was obtained by the following empirical equation:

$$R_E = (0.8433 * R^{0.6453} - 0.03324) \times 10^{(0.0332 * ET_o)} \quad (4)$$

Therefore, actual evapotranspiration (ETa) in each day of growing season was obtained based on the simulated canopy cover, water tensions and soil water balance (SWB).

$$ETa = Tr + E \quad (5)$$

2.2 Satellite Data Processing

For dealing with the necessity of considering the critical growth stages of a crop, four critical times take into

consideration including: I: initial canopy cover at the time of 90% crop emergence; II: time to maximum canopy cover; III: start of canopy senescence; and IV: time to maturity. Twenty-four days used for satellite imagery for each crop according to the four above-mentioned points are shown in Fig. 2.

The Level 1B moderate resolution imaging spectro-radiometer, *MODIS*, images of the Shahrekord plain are acquired to estimate daily evapotranspiration that covered the 2018–2019 growing season at the experimental site. Table 1 shows the details of *MODIS* products used in the study. The *MOD11 L2* data comprised of two thermal bands with a 1- km resolution and were used to estimate surface temperature and emissivity. Extraction of the binary file was performed for two visible (bands 1 and 2),

five short-wave infrared (bands 3, 4, 5, 6, and 7) and two thermal (bands 31 and 32) bands.

The original *MODIS* data were provided in hierarchical data format (HDF). The HDF is a multi-object file format for sharing scientific data in multi-platform distributed environments (Irmak and Kamble 2009). ArcGIS 10.2, ENVI 5, and ERDAS 9.1 were used to analyze the downloaded images. Individual images of each band were created for each day by converting their corresponding HDF files. *MODIS* land surface temperature (LST) product was downscaled to 250 m using a cubic convolution technique to be consistent with *MODIS* visible and near-infrared (*MOD09*) data (Irmak and Kamble, 2009).

SEBAL is based on the energy balance where sensible heat flux is related to temperature. SEBAL requires a number of computational steps to calculate the actual ET, as well

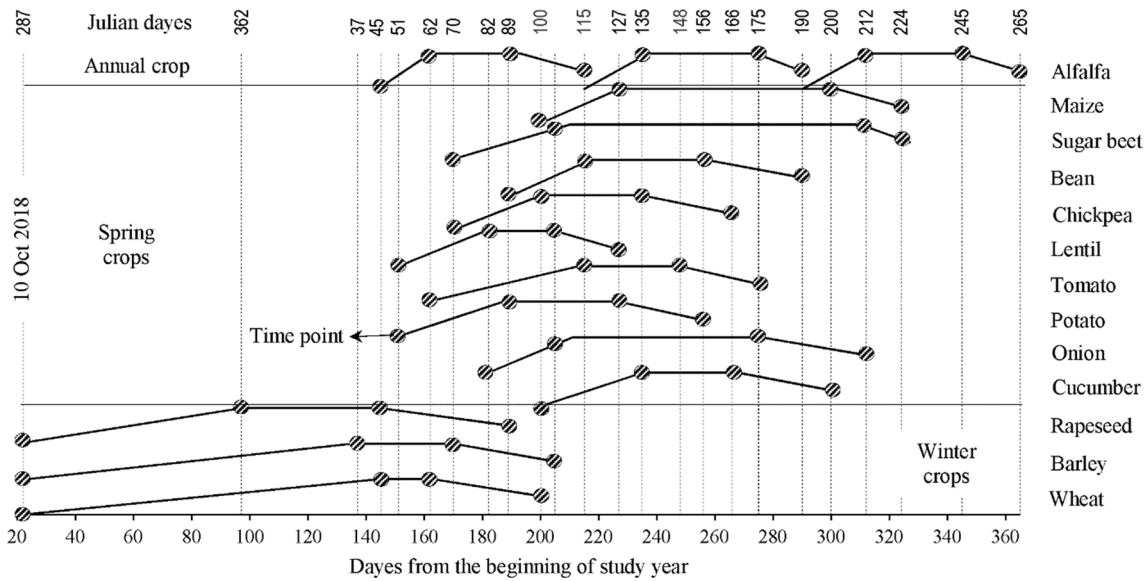


Fig. 2 Time points for estimating the actual evapotranspiration using SEBAL

Table 1 Details of MODIS products

MOD09	Band	Band width (nm)	Pixel size (m)
Visible	1	620–670	250
	2	841–876	
Near-infrared	3	459–479	500
	4	545–565	
	5	1230–1250	
	6	1628–1652	
	7	2105–2155	
MOD11		Band width (µm)	Pixel size (m)
Thermal	31	10.780–11.280	1000
	32	11.770–12.270	

as other energy exchanges between land and atmosphere, with the following input data (Bastiaanssen 2000): visible, near-infrared, and thermal infrared bands from MODIS and measurements of air temperature, relative humidity, wind speed, and solar radiation. Under the absence of advection, the energy balance in SEBAL is calculated at an instant time t for each satellite overpass by the following equation (Irmak and Kamble 2009):

$$\lambda ET = R_n - G - H \quad (6)$$

where λET is the latent heat flux which is the energy necessary to vaporize water (W m^{-2}); R_n is the net radiation (W m^{-2}), G is the soil heat flux (W m^{-2}) and H is the sensible heat flux (W m^{-2}). The net radiation flux (R_n) is calculated using the surface radiation balance:

$$R_n = (1 - \alpha)R_{s\downarrow} + R_{l\downarrow} - R_{l\uparrow} - (1 - \varepsilon_0)R_{l\downarrow} \quad (7)$$

where $R_{s\downarrow}$ is incoming shortwave, $R_{l\downarrow}$ is incoming longwave, and $R_{l\uparrow}$ is outgoing longwave radiation fluxes (W m^{-2}), ε_0 is the surface emissivity, and α is the surface albedo. G Index as a conduction flux through the soil matrix is driven by a thermal gradient in the uppermost topsoil. Heat flow varies with the state of the vegetation covering the soil that is influencing the light interception by the soil surface. SEBAL computes the ratio G/R_n near midday as:

$$\frac{G}{R_n} = \frac{T_s}{\alpha} (0.0038\alpha + 0.0074\alpha^2) (1 - 0.98NDVI^4) \quad (8)$$

where T_s is the satellite-derived surface temperature ($^{\circ}\text{C}$), and $NDVI$ is the normalized difference vegetation index (Eq. 8). The $NDVI$ is the ratio of the differences in reflectivities for the near-infrared band (NIR) and the red band (RED) to their sum:

$$NDVI = \frac{NIR - RED}{NIR + RED} \quad (9)$$

The sensible heat flux (H) is a convection flux through the atmosphere layers coming from the surface skin boundary layer with the topmost soil/vegetation layer:

$$H = \frac{\rho_{\text{air}} C_p dT}{r_{aH}} \quad (10)$$

where ρ_{air} is the density of moist air (kg m^{-3}), C_p is specific heat of air ($1004 \text{ J kg}^{-1} \text{ K}^{-1}$), dT is the vertical temperature difference between two heights ($z_0 = 0.1 \text{ m}$, and $z_s = 2 \text{ m}$) (K), and r_{aH} is the aerodynamic resistance to heat transfer (s m^{-1}). The dT is determined from the hot and cold pixels with assumed values of H (Bastiaanssen 2000). Selection of representative hot and cold pixels is extremely important for the accuracy of the ET estimations with SEBAL or with other models originated from SEBAL because the

model is calibrated based on the parameters from the two well-known locations (hot and cold pixels) for the entire image. The energy necessary to vaporize water (λET) under given atmospheric conditions is calculated as a residual of the energy balance components in Eq. (5). The instantaneous evaporative fraction (R) is used to express the ratio of the actual to the crop evaporative demand when the atmospheric moisture conditions are in equilibrium with the soil moisture conditions. Daily actual evapotranspiration (ET_{24}) is calculated from the daily averaged net radiation, Rn_{24} . The SEBAL model ignores G for time scales of 1 day or longer. Thus, net available energy ($Rn - G$) reduces to net radiation (Rn) at daily timescales. T_{24} is computed as:

$$ET_{24} = 86400 \frac{\lambda ET}{\lambda} \frac{Rn_{24}}{R_n} \quad (11)$$

where Rn_{24} is the 24-h averaged net radiation (W m^{-2}), k is the latent heat of vaporization (J kg^{-1}), and ET_{24} is daily actual ET (cm day^{-1}).

2.3 Study Area

The case study was conducted in Shahrekord plain during 2018–2019 season. Shahrekord plain located in $32^{\circ} 07'' \text{ N}$ to $32^{\circ} 35'' \text{ N}$ latitude and $50^{\circ} 38'' \text{ E}$ to $51^{\circ} 10'' \text{ E}$ longitude in Chaharmahal and Bakhtiari province, Iran (Fig. 3). The average annual precipitation is only 120 mm, which corresponds to semiarid conditions. Water shortage and agricultural demands are the main reasons for developing the decision-making framework for estimating the crop water requirement in this area. (Tabatabaei et al. 2010; Lalehzari et al. 2010; Fakharinia et al. 2012; Lalehzari et al. 2013, 2014; Lalehzari and Tabatabaei 2015).

3 Results and Discussion

The common crops selected to predict the canopy cover and transpiration in study area are summarized in Table 2. Moreover, the canopy cover used for estimating the transpiration in critical points is presented (Table 2). Canopy cover has the considerable role on the calculation of evaporation and transpiration. Evaporation values in the first period of growing season from sowing time to emergence completion are the major fraction of ET_a .

The actual evapotranspiration values calculated by SWB and SEBAL are compared in the Fig. 4. As shown in the figure and the scatter diagrams (together with calculated coefficient of determination), the accuracy of the SWB technique is satisfactory for predicting ET_a , because the recently obtained results are close to the previously obtained by SEBAL.

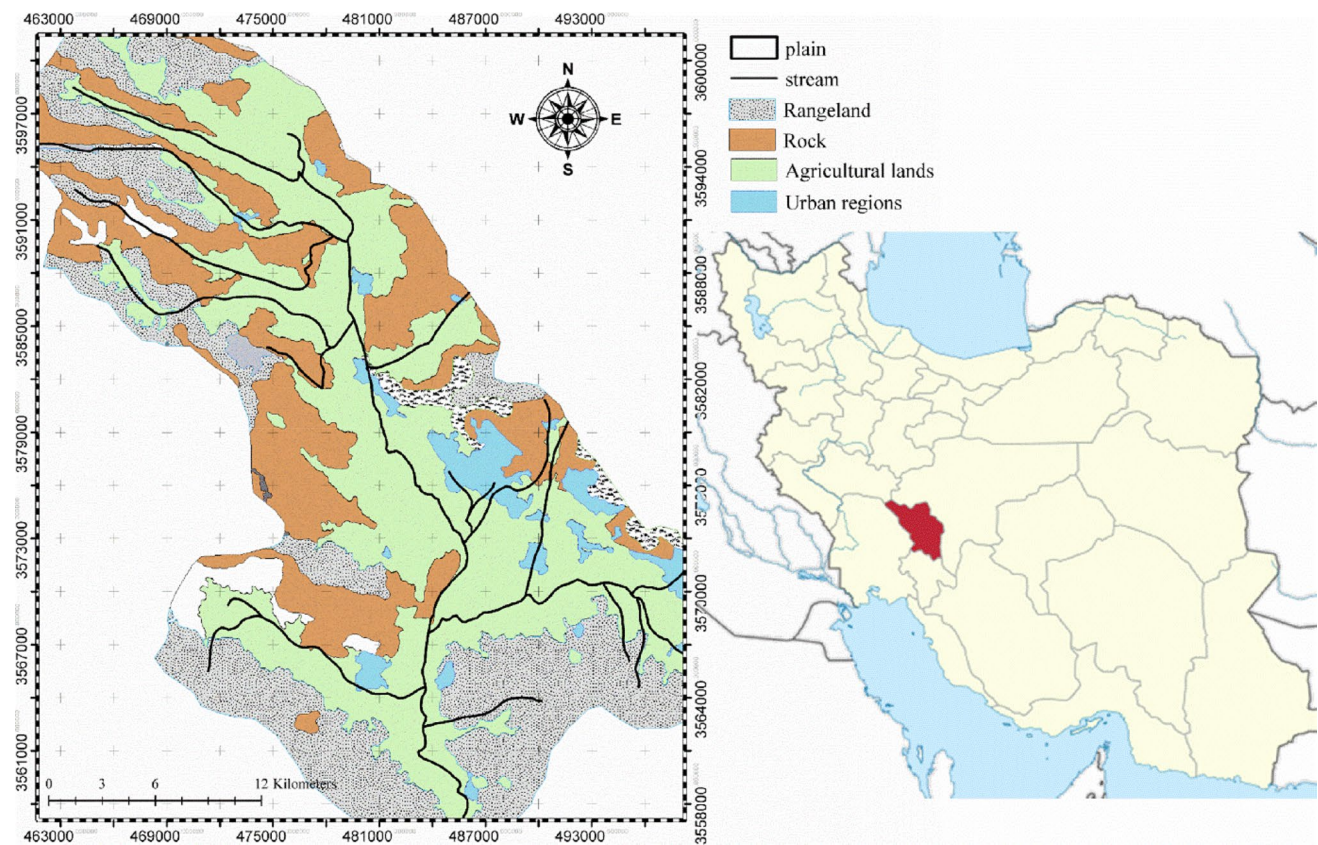


Fig. 3 The study area in Chaharmahal and Bakhtiari province, Iran

Table 2 Canopy cover in four critical stages of growing season

Crops	Emergence	Maximum canopy	Senescence	Maturity
	%	%	%	%
Wheat	4	93	89	87
Barley	6	91	89	87
Rapeseed	3	95	88	83
Lentil	2	81	68	67
Been	4	80	72	64
Chickpea	3	94	81	72
Tomato	6	76	50	45
Potato	4	77	44	37
Cucumber	3	81	75	60
Onion	2	84	60	44
Sugar beet	8	93	88	82
Maize	5	90	87	76

Alfalfa is a plant that has different growth periods and structures to simulate growth and calculate water requirements. Therefore, in this study, it was evaluated separately by applying special restrictions. Figure 5 shows a comparison between water requirements at ten points of the alfalfa

growing season. Results showed that at the beginning and end of the growing season, the two methods were more compatible with each other. Moreover, it seems to have been more accurate in periods when the role of evaporation outweighed transpiration.

The accuracy of the proposed methods could be evaluated by root mean square error, RMSE, and coefficient of residual mass, CRM (Lalezari and Boroomand-Nasab 2017).

$$RMSE = \pi \sqrt{\frac{\sum_{i=1}^n (ETa_{SEBAL} - ETa_{SWB})^2}{n}} \tag{12}$$

$$CRM = \frac{\sum_{i=1}^n (ETa_{SEBAL} - ETa_{SWB})_i}{\sum_{i=1}^n ETa_{SWB}} \tag{13}$$

where ETa_{SEBAL} and ETa_{SWB} are the calculated ETa using SEBAL and SWB, respectively, and n is the number of output data. Table 3 shows a summary of the evaluation results for crops and satellite images.

The RMSE has a minimum value of 0, with a better agreement close to 0. The coefficient of residual mass, CRM, indicates the underestimation and overestimation amounts by negative and positive values, respectively. According to the

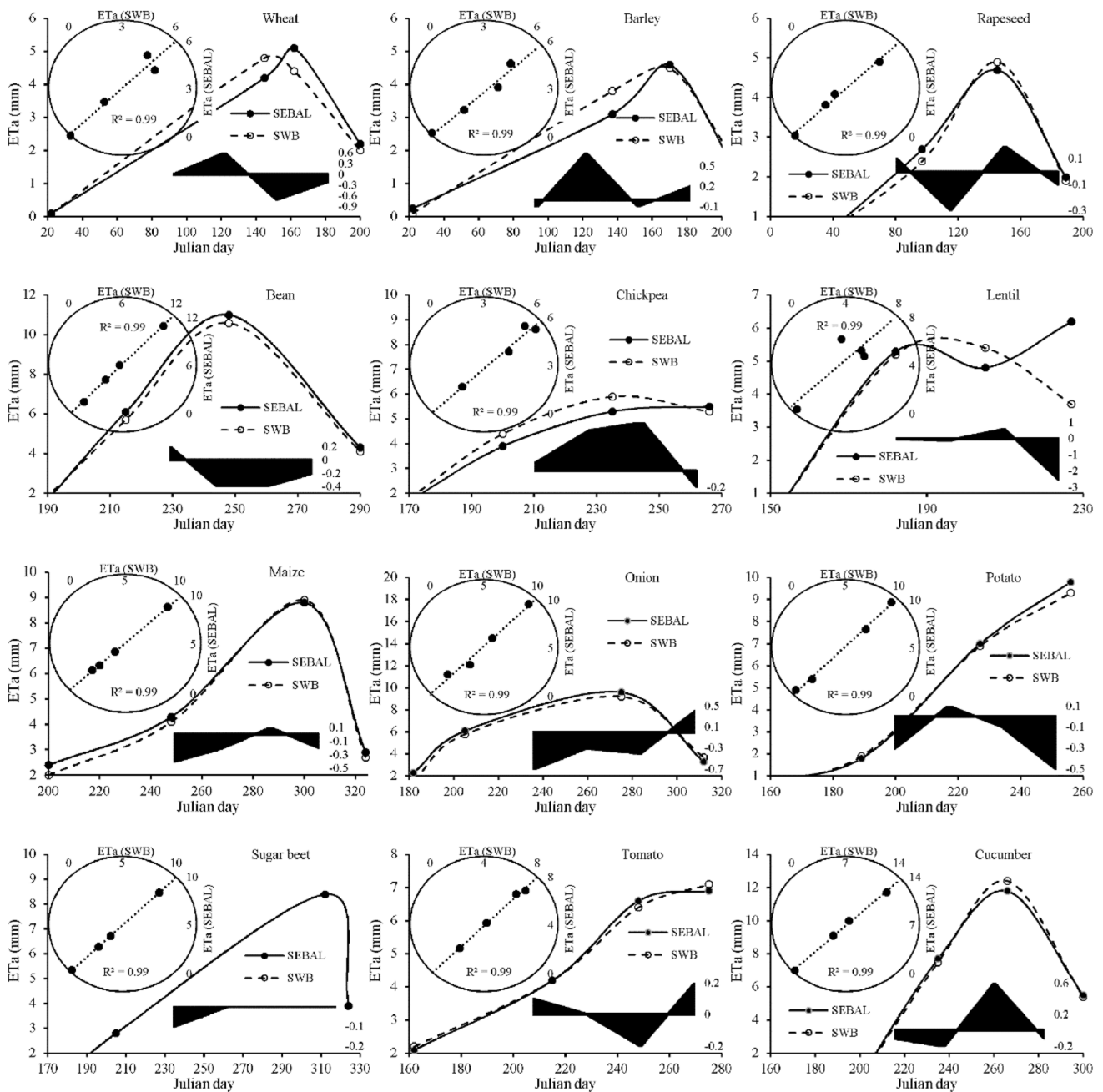


Fig. 4 Comparison between calculated ETa using SEBAL and SWB methods

table, daily ETa predicted based on the SEBAL method are underestimated for barley, cucumber, chickpea, and alfalfa and overestimated for wheat, potato, onion, lentil, bean, and maize and are close to the calculated values of SWB for tomato, colza, and sugar beet.

4 Summary and Conclusion

In this study, the remote sensing images as a data source for agricultural water modeling and soil water balance components were considered to estimate the actual

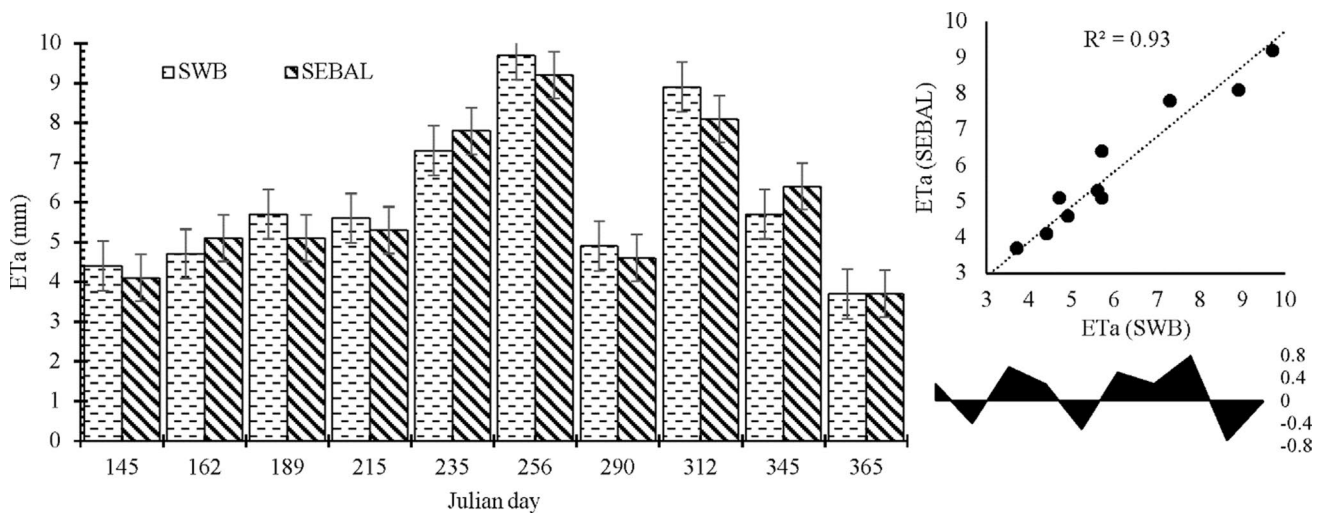


Fig. 5 Calculated actual evapotranspiration of alfalfa using SEBAL and SWB methods

Table 3 Comparison with the soil water balance and *SEBAL* algorithm for estimating the *ETa*

Crops	RMSE	CAM	Julian days	RMSE	CAM	Julian days	RMSE	CAM
Wheat	0.47	0.03	287	0.10	0.13	127	1.77	0.25
Barley	0.38	-0.06	362	0.30	0.13	135	0.47	0.00
Tomato	0.15	-0.01	37	0.70	-0.18	148	0.28	0.04
Potato	0.30	0.04	45	0.40	-0.08	156	0.50	0.00
Onion	0.47	0.05	51	0.21	0.38	166	0.45	-0.02
Cucumber	0.32	-0.01	62	0.47	0.09	175	0.32	0.01
Colza	0.19	0.01	70	0.10	0.02	190	0.25	-0.01
Lentil	1.29	0.14	82	0.50	0.12	200	0.10	0.00
Chickpea	0.41	-0.06	89	0.32	-0.07	212	0.52	-0.06
Bean	0.32	0.04	100	0.34	0.02	224	0.14	0.03
Sugar beet	0.05	0.01	105	0.35	-0.03	245	0.70	0.12
Maize	0.25	0.05	115	0.29	0.01	265	0.00	0.00
Alfalfa	0.49	-0.02	Total satellite images and cropping pattern				0.49	0.01

evapotranspiration. SEBAL technique was applied to characterize the surface energy balance for predicting the evapotranspiration, and then, the derived *ETa* was compared with results obtained by a calibrated framework of soil, water, and crop relationships. Preliminary results obtained by applying SWB and SEBAL show a good agreement between the both estimated evapotranspiration fluxes. According to the coefficient of residual mass index, actual evapotranspiration in daily time steps predicted based on the SEBAL method is underestimated for barley, cucumber, chickpea, and alfalfa and overestimated for wheat, potato, onion, lentil, bean, and maize and are close to the calculated values of SWB for tomato, colza, and sugar beet.

Due to the fact that the SWB method is based on step-by-step mathematical calculations, it is more efficient in computer models and optimization than remote sensing.

Furthermore, the time required to estimate SWB transpiration is much less than other experimental and physical methods.

Acknowledgements Scientific Research Fund of Education Department of Yunnan Province, No. 2020J1028.

References

Akbari M, Toomanian N, Droogers P, Bastiaanssen W, Gieske A (2007) Monitoring irrigation performance in Esfahan, Iran, using NOAA satellite imagery. *Agric Water Manage* 88:99–109

Allen RG, Tasumi M, Trezza R (2007) Satellite-based energy balance for mapping evapotranspiration with internalized calibration (METRIC)-Model. *J Irri Drain Eng* 133(4):380–394

Balugani E, Lubczynski MW, Metselaar K (2016) A framework for sourcing of evaporation between saturated and unsaturated zone in bare soil condition. *Hydrol Sci J* 61(11):1981–1995

- Balugani E, Lubczynski MW, Reyes-Acosta L, van der Tol C, Francés AP, Metselaar K (2017) Groundwater and unsaturated zone evaporation and transpiration in a semi-arid open woodland. *J Hydrol* 547:54–60
- Bastiaanssen WGM (2000) SEBAL based sensible and latent heat fluxes in the irrigated Gediz Basin. *Turkey J Hydrol* 229:87–100
- Chemin Y, Platonoy A, UI-Hassan M, Abdullaey I (2004) Using remote sensing data for water depletion assessment at administrative and irrigation system levels. *Agric Water Manage* 64(3):183–196
- Chen JM, Chen X, Ju W, Geng X (2005) Distributed hydrological model for mapping evapotranspiration using remote sensing inputs. *J Hydrol* 305:15–39
- Colak YB, Yazar A, Colak I, Akca H, Duraktekin G (2015) Evaluation of crop water stress index (CWSI) for eggplant under varying irrigation regimes using surface and subsurface drip systems. *Agric Sci Procedia* 4:372–382
- Fakharinia M, Lalehzari R, Yaghoobzadeh M (2012) The use of subsurface barriers in the sustainable management of groundwater resources. *World Appl Sci J* 19(11):1585–1590
- Fallah-Mehdipour E, Bozorg Haddad O, Marino MA (2013) Extraction of multi-crop planning rules in a reservoir system: application of evolutionary algorithms. *J Irrig Drain Eng.* [https://doi.org/10.1061/\(ASCE\)IR.1943-4774.0000572](https://doi.org/10.1061/(ASCE)IR.1943-4774.0000572)
- Fry LM, Apps D, Gronewold AD (2020) Operational seasonal water supply and water level forecasting for the Laurentian great lakes. *J Water Resour Plan Manage* 146(9):04020072
- Hsiao TC, Steduto P, Fereres E (2007) A systematic and quantitative approach to improve water use efficiency in agriculture. *Irrig Sci* 25:209–231
- Ines AVM, Honda K, Gupta AD, Droogers P, Clemente RS (2006) Combining remote sensing-simulation modeling and genetic algorithm optimization to explore water management options in irrigated agriculture. *Agric Water Manage* 83:221–232
- Irmak A, Kamble B (2009) Evapotranspiration data assimilation with genetic algorithms and SWAP model
- Lalehzari R, Boroomand-Nasab S (2017) Improved volume balance using upstream flow depth for advance time estimation. *Agric Water Manage* 186:120–126
- Lalehzari R, Kerachian R (2020) Developing a framework for daily common pool groundwater allocation to demands in agricultural regions. *Agric Water Manage* 241:106278
- Lalehzari R, Tabatabaei SH (2015) Simulating the impact of subsurface dam construction on the change of nitrate distribution. *Environ Earth Sci* 74:3241–3249
- Lalehzari R, Tabatabaei SH, Kholghi M (2010) Hydrodynamic coefficients estimation and flow treatment prediction in Shahrekord aquifer using PMWIN model. In: 14th International Water Technical Conference Cairo, Egypt
- Lalehzari R, Tabatabaei SH, Kholghi M (2013) Simulation of nitrate transport and wastewater seepage in groundwater flow system. *Int J Environ Sci Technol* 10:1367–1376
- Lalehzari R, Tabatabaei SH, Kholghi M, Yarali N, Saba AA (2014) Evaluation of Scenarios in artificial recharge with treated wastewater on the quantity and quality of Shahrekord aquifer. *J Environ Stud* 40(1):52–55
- Lalehzari R, Boroomand-Nasab S, Moazed H, Haghighi A (2016) Multi-objective management of water allocation to sustainable irrigation planning and optimal cropping pattern. *J Irrig Drain Eng.* [https://doi.org/10.1061/\(ASCE\)IR.1943-4774.0000933](https://doi.org/10.1061/(ASCE)IR.1943-4774.0000933)
- Lalehzari R, Boroomand-Nasab S, Moazed H, Haghighi A, Yaghoobzadeh M (2020) Simulation-optimization modeling for water resources management using NSGAI-OIP and Modflow. *Drain, Irrig.* <https://doi.org/10.1002/ird.2424>
- Li Y, Kinzelbach W (2020) Resolving conflicts between irrigation agriculture and ecohydrology using many-objective robust decision making. *J Water Resour Plan Manage* 146(9):05020014
- Mahan JR, Young AW, Payton P (2012) Deficit irrigation in a production setting: canopy temperature as an adjunct to ET estimates. *Irrig Sci* 30:127–137
- Maroufpoor S, Maroufpoor E, Bozorg-Haddad O, Shiri J, Mundher Yaseen Z (2019) Soil moisture simulation using hybrid artificial intelligent model: hybridization of adaptive neuro fuzzy inference system with grey wolf optimizer algorithm. *J Hyd.* <https://doi.org/10.1016/j.jhydrol.2019.05.045>
- Mason L (2019) A new transboundary hydrographic dataset for advancing regional hydrological modeling and water resources management. *J Water Resour Plan Manage* 145(6):06019004
- Omidzade F, Ghodousi H, Shahverdi K (2020) Comparing fuzzy SARSA learning and ant Colony optimization algorithms in water delivery scheduling under water shortage conditions. *J Irrig Drain Eng* 146(9):04020028
- Parsinejad M, Bemani Yazdi A, Araghinejad S, Nejadhashemi AP, Sarai Tabrizi M (2013) Optimal water allocation in irrigation networks based on real time climatic data. *Agri Water Manage* 117:1–8
- Raes D, Steduto P, Hsiao TC, Fereres E (2017) FAO crop-water productivity model to simulate yield response to water. *Food and Agriculture Organization of the United Nations, Rome*
- Reyes-Acosta J, Lubczynski M (2011) Spatial assessment of transpiration, groundwater and soil-water uptake by oak trees in dry-season at a semi-arid open-forest in Salamanca, Spain. In: Martínez Fernández and Sánchez Martín (Eds.), pp 65–70
- Sang X, Zhao Y, Zhai Z, Chang H (2019) Water resources comprehensive allocation and simulation model (WAS). *Appl Chin J Hydraul Eng* 50(2):201–208
- Sun Q, Xu G, Ma C, Chen L (2017) Optimal crop-planting area considering the agricultural drought degree. *J Irrig Drain Eng* 143(12):04017050
- Tabatabaei SH, Lalehzari R, Nourmahnad N, Khazaei M (2010) Groundwater quality and land use change (A case study: shahrekord aquifer, Iran). *J Res Agric Sci* 6:39–48
- Vedula S, Mujumdar PP, Sekhar GC (2005) Conjunctive use modeling for multicrop irrigation. *Agric Water Manage* 73:193–221
- Varzi M, Trout TJ, DeJonge KC, Oad R (2019) Optimal water allocation under deficit irrigation in the context of Colorado Water Law. *J Irrig Drain Eng* 145(5):0015634
- Veysi S, Naseri AA, Hamzeh S, Bartholomeus H (2017) A satellite based crop water stress index for irrigation scheduling in sugarcane fields. *Agric Water Manage* 189:70–86
- Yan Z, Zhou Z, Sang X, Wang H (2018) Water replenishment for ecological flow with an improved water resources allocation model. *Sci Total Environ* 643:1152–1165
- Yan Z, Zhou Z, Liu J, Wen T, Sang X, Zhang F (2020) Multiobjective optimal operation of reservoirs based on water supply, power generation, and river ecosystem with a new water resource allocation model. *J Water Resour Plan Manage* 146(12):05020024
- Yao Y, Zheng C, Tian Y, Li X, Liu J (2018) Eco-hydrological effects associated with environmental flow management: a case study from the arid desert region of China. *Ecohydrology* 11(1):e1914. <https://doi.org/10.1002/eco.1914>